# 9

# Synergistic Noise-By-Flow Control Design of Blade-Tip in Axial Fans: Experimental Investigation

Stefano Bianchi[1], Alessandro Corsini[1] and Anthony G. Sheard[2]
[1]*Sapienza University of Rome,*
[2]*Flakt Woods Ltd,*
[1]*Italy*
[2]*UK*

## 1. Introduction

The increasing concern on noise emission had recently inspired the definition of a regulatory framework providing standards on eco-design requirements for energy-using products and noise levels, i.e. the European Directive 2005/32/EC (European Parliament, 2005). The compliance to standards within the fan industry appears more stringent than for other sectors because of their use in ventilation systems entailing the direct human exposure to noise emission. This driver demands the elaboration of fan design solutions and technologies in which the exploitation of noise control strategies must not affect aerodynamic performances.

To summarise, the main generation mechanisms of aerodynamic noise in low-speed axial fans are: turbulent inflow, self noise (turbulent or laminar boundary layers, boundary layer separation), trailing edge noise, secondary flows (Fukano *et al*., 1986), and tip leakage related noise.

Among these aerodynamic phenomena, Inoue and Kuroumaru (1989), Storer and Cumpsty (1991) and Lakshminarayana *et al*. (1995) investigated the role of tip leakage flows in compressor rotors and demonstrated the three-dimensional and unsteady nature, and the influence on aerodynamic losses and noise generation. In the context of low-speed turbomachines, Akaike *et al*. (1991) pointed out that the vortical structure near the rotor tip in industrial fans is one of the major noise generating mechanisms. The tip leakage noise can be one of the most significant sources correlated to the broadband spectral signature (Longhouse, 1978; Fukano *et al*., 1986; Kameier & Neise, 1997). Kameier and Neise (1997) highlighted that, in addition to the broadband influence, tip leakage flows could be responsible for narrowband tones at frequencies below the blade passing frequency in coincidence with a tip vortex separation.

During the last decades, noise control has emerged as a new field of research as the literature demonstrates (Gad-el-Hak, 2000; Joslin *et al*., 2005), and scholars have proposed noise reduction strategy classifications, which distinguish between passive, active and reactive devices. A number of research programmes envisioned designs tailored to a synergistic noise and flow control by incorporating structural (passive) or flow (active)

technologies in synergy with those mechanisms leading to a reduction of the noise sources' effectiveness. Two textbook examples of this include: i) the chevron mixer for jet noise reduction among the structural-passive technology (Saiyed *et al.*, 2000), and ii) the trailing edge blowing in turbomachinery noise suppression in the active-flow technology family (Brookfield & Waitz, 2000).

According to Thomas *et al*. (2002) and Joslin *et al*. (2005), we can base a possible classification of flow and noise control technologies on the nature of the linkage between the underlying flow physics and the noise generation mechanisms. According to the exploitation of the flow control, the overall effect on performance or noise can be productive, due to the direct or indirect linkages, or counterproductive (Joslin *et al*., 2005).

In the framework of industrial turbomachinery, the noise control techniques documented in the open literature are mostly passive systems**.** In terms of the flow to noise control relationship, we can regard them as exploiting a direct linkage targeting the flow features responsible for a significant noise generation. Researchers mostly base the passive or preventive control concepts on the rotor's (blade's) geometrical characteristics or its environment (casing) to control the generation mechanisms and the fluctuating forces without sacrificing aerodynamic performance. Researchers usually accomplished this goal by either reducing the leakage flow rate or by enhancing the primary-secondary flow momentum transfer. Researchers first reported casing treatments in the shroud over compressor blades in the early 1970s and with grooves (Takata & Tsukuda, 1977; Smith & Cumpsty, 1984), and stepped tip gaps (Thompson *et al*., 1998). They found them to improve the stable operating range by weakening the tip leakage flow. In his pioneering work, Longhouse (1978) introduced rotating shrouds attached to the rotor tips to reduce tip leakage vortex noise, implying that the vortical flow near the tip is closely related to the fans' noise characteristics as well as the aerodynamics. Specifically associated with fan technology, researchers have proposed recirculating vanes and annular rings as anti-stall devices (Karlsson & Holmkvist, 1986) which commercial applications routinely utilise today. When examining the rotor blade tip, a number of contributions demonstrated the viability of anti-vortex appendages such as Quinlan and Bent's (1998) investigations, or by industrial patents for ventilating fans (Karlsson & Holmkvist, 1986; Longet, 2003; Mimura, 2003; Uselton *et al*., 2005). Recent systematic numerical and experimental research efforts have renewed the interest on the incorporation of flow and structural control methodologies in blade design to reduce noise emission. Akturk & Camci (2010) reported a programme of work on novel tip platform extensions for energy efficiency and acoustic gains, in view of the implementation of the control capability on tip leakage swirl to ducted lift fans for vertical take-off and landing applications (Akturk and Camci, 2011a, b).

Corsini and co-workers (Corsini & Sheard, 2007; Corsini *et al*., 2007; Bianchi *et al*., 2009b, c) investigated the application of profiled end plates to the blade tips on compact cooling fans. They based the novel design concept on the shaping of end-plates according to the control of chord-wise evolution of leakage vortex rotation number (Corsini & Sheard, 2007; Corsini *et al*., 2007).

This chapter outlines new concepts for the design of blade tip end-plate in subsonic axial fan rotors based on the tip leakage vortex control. Because of the role that organised structures in turbulent flow could play in the noise generation process, controlling these eddies may be one of the keys to noise suppression (Ffowcs Williams, 1977). Experimental and numerical studies proved the pay-off resulting from the adoption of tip leakage flow control

technologies (Bianchi *et al*., 2009b, c; Corsini *et al*., 2010), and the authors speculated about the role of leakage vortex bursting phenomenon on the aerodynamic and aeroacoustic performance of such a fan class. The vortex breakdown is an intriguing and practically important phenomenon occurring in swirling flows, and depending on the application, could be a productive or counter-productive flow feature. For this reason, scholars have been interested in its control for two decades. This is an active research area that primarily the aeronautics field continues to explore, for example delaying delta wing vortices or accelerating trailing tip vortices (Spall *et al*., 1987), and studying combustor, valve or cyclone behaviour (Escudier, 1987). The proposed design concept rationale advocates the linkage between the end-plate's chordwise shape and the augmentation-diminution of tip leakage vortex near-axis swirl (Jones *et al*., 2001; Herrada & Shtern, 2003). Reconfiguring the end-plate at the tip implements the exploitation of this direct noise-by-flow control in order to influence the momentum transfer from the leakage flow and to force some waviness into the leakage vortex trajectory, as the delta-wing platform design (Srigrarom & Kurosaka, 2000) also shows. The authors have deliberately designed the variation of thickness to control the chordwise evolution of the leakage vortex rotation number, here chosen as the metric for the vortex swirl level. The different design criteria under scrutiny (Corsini & Sheard, 2007, 2011; Corsini *et al*., 2009a) are intended to control the leaked flow and to induce a subtraction-addition of near-axis momentum to the tip vortex. As such, the new end-plate design concepts comprise passive control of tip vortex swirl level to enhance the mixing of coherent tip vortical structures with a favourable correlated sound field modulation (Corsini *et al*., 2009a; Corsini and Sheard, 2011).

Section 2 describes the test fans. Section 3 illustrates the rationale of the proposed end-plate thickness distribution concepts. Section 4 presents the experimental methodology that the authors used in the investigation, while Section 5 illustrates the comparative assessment of the end-plate aerodynamics and aeroacoustics to prove the technical merits of a passive control strategy for controlling leakage flow and rotor-tip self noise. The chapter concludes, in Section 6, with a discussion of the findings and a summary of the major conclusions.

## 2. Axial fans

The authors conducted the present research on a family of commercially available cooling fans. The in-service experiences indicated that this family of fans gives good acoustic performance with respect to the state-of-the-art configurations. The modified ARA-D type blade sections were single-parameter airfoils originally conceived for propellers. Clearance between the blade tips and the casing was constant at 1% of blade span. The impeller had a mechanism for varying the blade-pitch angle to customise the load, airflow, and stalling properties. Table 1 shows the blade profiles geometry and the fan rotor specifications. Data in Table 1 refer to the *datum* fan family, coded AC90/6.

The authors operated the fan in a custom-built casing made from rings of cast and machined steel. The studied blade configurations, for *datum* and rotors fitted with tip end-plates, feature a high tip pitch angle, i.e. 28 degrees, measured, as is customary in industrial fan practice, from the peripheral direction. The authors selected this angular setting which corresponds to the fan unit peak performance. Notably, the datum fan features a peak pressure rise of about 300 Pa at 5 $m^3/s$ with a design pressure rise of point of 270 Pa at 7 $m^3/s$ and 0.77 of total efficiency.

| | *AC90/6 datum fan* | |
|---|---|---|
| *Blade geometry* | *hub* | *tip* |
| $\ell / t$ | 1.32 | 0.31 |
| *stagger angle (deg)* | 54 | 62 |
| *camber angle (deg)* | 46 | 41 |
| *Rotor specifications* | | |
| *blade count* | 6 | |
| *blade tip pitch angle (deg)* | 28 | |
| *hub diameter $D_h$ (mm)* | 200.0 | |
| *casing diameter $D_c$ (mm)* | 900.0 | |
| *rotor tip clearance $\tau$ (% span)* | 1.0 | |
| *rated rotational frequency (rpm)* | 900 – 950 | |

Table 1. AC90/6 fan family specifications. *Datum* blade geometry and rotor specifications

## 3. Design of tip end-plates for noise-by-flow control

### 3.1 Background studies on tip leakage vortex

Corsini and Sheard (2007) and Corsini *et al.* (2007, 2010) have assessed the performance gains related with the development of end-plate technology, consisting of constant thickness end-plate originally designed at Fläkt Woods Ltd for an industrial fan designated AC90/6/TF. The authors studied numerically the leakage flow evolution to isolate the mechanisms that govern the improvement in the aeroacoustic signature. The numerical investigation tool was based on an original parallel Finite Element flow solver (Corsini et al., 2005). Despite the steady-state conditions (Corsini *et al.*, 2007, 2010), RANS was adopted as an effective tool for this investigation because it is capable of capturing details of the vortex structures at the tip (Escudier & Zehnder, 1982, Inoue & Furukawa, 2002). One of the main findings was that in rotor AC90/6/TF, the leakage flow control that the aerodynamic appendages at the blade tip gave rise along the operating line, in the near-design operation, to a tip leakage vortex bursting.

A multi-criteria analysis assessed the occurrence of tip leakage vortex breakdown in the state-of-the-art fan rotor (Corsini *et al.*, 2010). First, the visualization of three-dimensional streamlines at the tip revealed the presence of a large bubble-type separation with the flow reversal being indicative of the critical bursting phenomenon (Lucca-Negro & O'Doherty, 2001). According to Leibovich (1982), the appearance of the vortex bursting in the bubble form can be interpreted as a consequence of a sufficiently large swirl level and this form of the vortex breakdown is increasingly steady with the level of swirl (Escudier & Zehnder, 1982, Inoue & Furukawa 2002). Second, the presence of a stagnation point along the vortex axis indicated the onset of the vortex collapse in accordance with the observation of Spall et al. (1987), who first identified it as a necessary condition for the breakdown to appear. As a last criterion, the most distinctive feature was the tip leakage vortex helicity inversion occurring as a result of the counter-rotation of the vortex exiting from the bursting region, accepted as evidence of vortex breakdown in compressor rotors (Inoue & Furkawa, 2002). In particular this evidence could be interpreted, according to Leibovich (1982) explanation of the vortex breakdown on the basis of the behaviour of the azimuthal vortex component, as a consequence of a change in the angle between the velocity and vortex vectors.

In order to suppress the tip leakage vortex-bursting phenomenon in the fan rotor fitted with a base-line tip feature, the authors proposed new end-plate design concepts to exploit a passive control on vortex breakdown formation (Corsini & Sheard, 2007, 2011).

### 3.2 Variable thickness end-plate design concept

The *Variable Thickness End-plate* design concept accomplishes the control on vortex breakdown onset advocating the use of a chordwise variation, in particular diminution, of the end-plate thickness. The authors designated the fan rotor fitted with this end-plate geometry as AC90/6/TFvte.

To suppress the tip-leakage vortex-bursting phenomenon in the operation of the AC90/6/TF fan rotor, the authors recently proposed a new end-plate design concept. The proposed configuration controls vortex breakdown by means of an end-plate of variable chord-wise thickness. The first improved concept's aim was to enhance near-axis swirl ((Jones *et al.*, 2001; Herrada & Shtern, 2003) by reconfiguring the end-plate at the tip with a view to influencing the momentum transfer from the leakage flow and to force some waviness into the leakage-vortex trajectory. According to the analysis of tip-leakage vortices in terms of a Rossby number based swirl metric (Spall *et al.*, 1987), the end-plate's shape depends on the definition of a safe rotation number chordwise gradient. The investigation's rationale was to compute the end-plate thickness distribution by combining a simplified law for the tip-gap pressure drop with a stability criterion of tip leakage vortex prescribed by the vortex rotation's safe chordwise distribution or Rossby number.

Notably, as Corsini *et al.* (2009b) also explained, the adoption of variable thickness end-plate resulted in improved pressure rise capability and efficiency owing to the control on tip vortex bursting. The counterpart of this aerodynamic pay-off was that the presence of leakage related organised vortical structure in TFvte end-plate associated with a slightly higher sound A-filtered power level SWL.

### 3.3 Multiple vortex-breakdown end-plate design concept

In accordance with the background experiences on tip leakage vortex swirl behaviour, the second end-plate design criterion, named *Multiple Vortex Breakdown*, advocates the linkage between the end-plate geometry and the modulation of tip leakage vortex near-axis swirl. We can interpret this direct linkage flow-to-noise control by deliberately designing the shape of the end-plate at the tip to control the chordwise evolution of the leakage vortex rotation number.

The design criterion is to control the leaked flow in order to induce a sequence of subtraction of momentum transfer to the tip vortex up to a near-critical condition, followed by an addition of near-axis momentum (Corsini *et al.*, 2009a). As such, the new end-plate design concept exploits a passive control of tip vortex swirl level based on a succession of breakdown or bursting conditions able to enhance the mixing of coherent tip vortical structures with a favourable modulation of the correlated sound field.

The rationale is to derive an explicit correlation among the tip end-plate thickness, the tip vortex kinematics, the local blade loading, and the magnitude of the leakage flow. In the vein of the flow mechanism under control, which we base on the modulation of the tip vortex rotation number, the authors built the analytical law for the end-plate geometry advocating the definition of the Rossby number as the problem's key metric.

### 3.4 Tip end-plate aerodynamics

To complete the illustration of the passive noise concepts, Figure 1 outlines the main background findings on improved tip design. In detail, Figure 1.a shows the chordwise distribution of the tip leakage vortex swirl level at design condition. The authors selected the Rossby number Ro swirl metric definition in acccordance with the interpretive criterion on vortex breakdown Ito and co-workers (1985) proposed. The figure gives the evolution of the Rossby number on the chord fraction for four different end-plate configurations, namely the base-line with constant thickness (AC90/6/TF), the variable thickness end-plate (AC90/6/TFvte) and the MVB end-plate design (AC90/6/TFmvb) plotted against the *datum* one. Moreover, Figure 1.b shows a sketch of the blade tip for the AC90/6 class of fan unit.

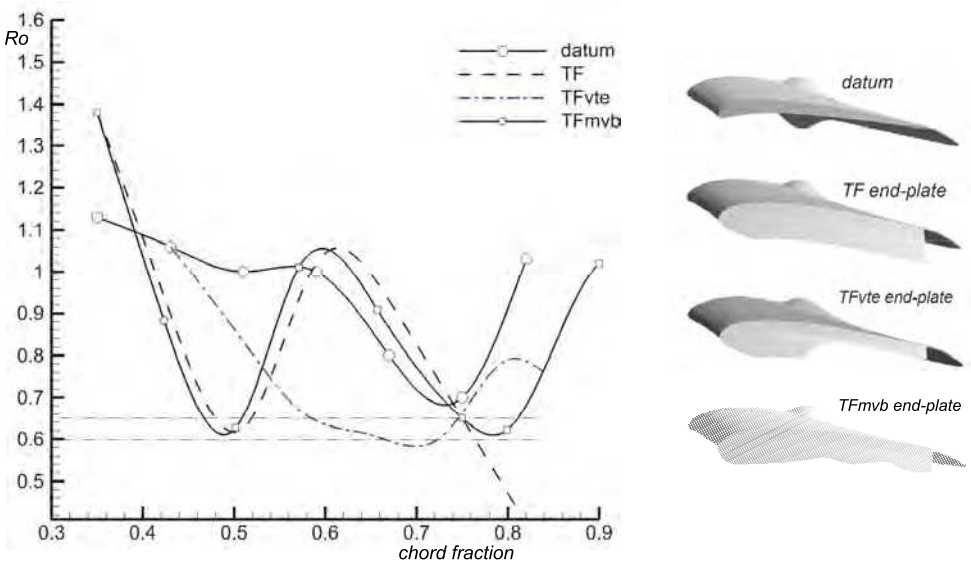


Fig. 1. Background on improved tip concepts, chordwise evolution of tip leakage vortex Rossby number (left), and end-plate geometries (right)

The Ro distributions, Figure 1 (left), indicate that the AC90/6/TF fan features a vortex breakdown in coincidence with the attainment of the Rossby number's critical value. The critical Ro number values that the open literature mentions range from 0.64 for the breakdown of a confined axi-symmetric vortex (Uchida *et al.*, 1985), to 0.6 for wing tip vortices with bubble or spiral type vortex breakdown (Garg & Leibovich, 1979). Figure 1 (right) depicts the end-plate geometries (Corsini & Sheard, 2007, 2011).

#### 3.4.1 Fan performance

The main performance parameters were the fan total pressure and the efficiency. The authors measured the static and dynamic pressure for this study in the Fläkt Woods test rig at Colchester (UK). They based the performance measurements on pressure taps, equally spaced on the casing wall, and a standard Pitot-probe. The authors mounted the probe on a traverse mechanism fixed to the test rig's outer wall. The Furness digital multi-

channel micro-manometer (Model FC012, Furness Controls Ltd, UK) had 2 kPa range and a resolution of 1 Pa on pressure data. The pressure measurements accuracy was ± 0.5% of read data. The authors calculated the efficiency as the ratio between the air power (computed on either static or dynamic pressure rise) and the electric power. They measured the absorbed electric power with an AC power analyser with an accuracy of 0.24% of read data.
Figure 2 plots the curves of the total pressure and the efficiency based on total pressure for the datum fan rotor.

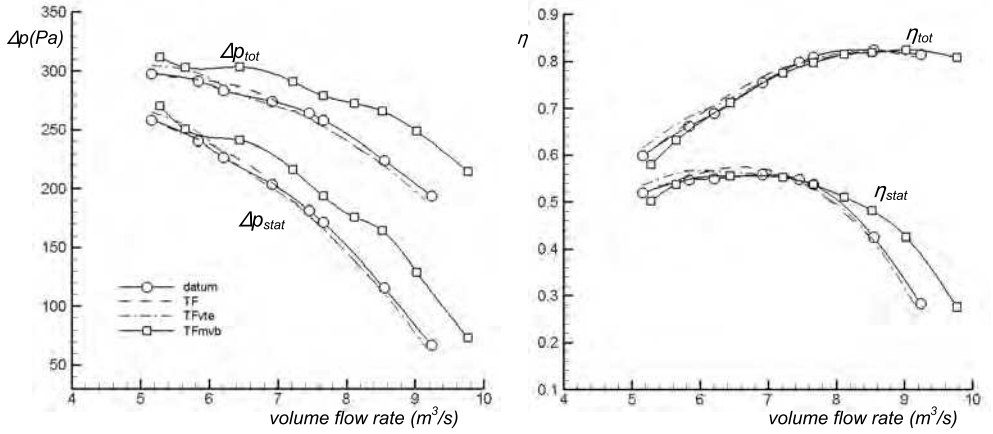


Fig. 2. Measured pressure (left) and efficiency (right) characteristic curves

## 4. Methodology

### 4.1 Noise measurements

The authors designed this study's methodology to achieve the following specific objectives: (i) to characterise the azimuthal distribution of the radiated sound pressure level (Lp) of the various fan-blade configurations; and (ii) to investigate the directivity of the Lp spectra and (iii) speculate about the aerodynamic origins of the noise. In pursuit of these aims, the study measured the azimuthal far-field fan noise radiated from the exhaust flow according to the BS848-2.6:2000 standard (ISO 2000), which is equivalent to the ISO 10302:1996 standard.
The authors conducted the experiments in the Fläkt Woods anechoic chamber at Colchester (UK). The chamber is an anechoic facility for noise emission certification according to the BS848-2.6:2000 standard (ISO 2000). The anechoic chamber cut-off frequency is 25 Hz. Bianchi *et al.* (2009a) report additional details on the experimental setting. The authors conducted measurements at the fan exhaust. Table 2 gives the main specifications of the near- and far-field probes.
The authors acquired microphone signals with a 01-dB Symphonie digital signal processor. In all cases, the authors measured signals for $2.85 \times 10^4$ rotor revolutions. The balancement of rotors ensures a vibration peak no greater than 4 mm/s.

| | |
|---|---|
| *Pre-amplifier* | Brüel & Kjær equipment connected to a 2 channels Symphonie acquisition system |
| *Near-field microphone* | GRAS 40AG |
| Diameter | 2.7 mm |
| Frequency range | 0 Hz – 20 kHz |
| Sampling frequency | 50 kHz |
| Dynamic range | 27 dB – 160 dB |
| *Far-field microphone* | Brüel & Kjær 4954 |
| Frequency range | 0 Hz – 20 kHz |
| Sampling frequency | 50 kHz |
| Dynamic range | Up to 165 dB |
| *Sound analyser* | 01dB-Metravib dBFA Suite |

Table 2. Specifications of the near- and far-field microphones

The authors operated the fan in a custom-built casing made from cast and machined steel rings. Clearance between the blade tips and the casing was constant at 1% of blade span. The authors used a 2.5-kW, direct coupled-induction 400-volt (AC), 3-phase CM29 motor to drive the rotor at a constant speed of 945±5 rpm. The blade tip's speed was 44.3 m/s. Under these conditions, the blade-passing frequencies (BPFs) for all the tested configurations were in the range 93.75±3.125 Hz. To isolate the aerodynamic noise, the authors conducted a preliminary motor test to establish its spectral signature so as to allow for a correction of subsequent noise measurements. In all cases, the authors measured the signals for 30 s. They repeated each measurement three times. The error was in the range of 0.1-0.2 dB at 1kHz, as given by the calibration certification on the microphones and the acquisition system according to ISO IEC60651. Figure 3 shows a photograph of the test-rig, together with the set-up of the near- and far-field probes.

The authors installed the fan downstream from the plenum chamber, using a type-A configuration, with a free inlet blowing on the motor and on the four struts, as is customary for the in-service operation. They mounted a bell-mouth on the fan inlet. The shape of this bell-mouth was aerodynamically optimised to give uniform and unseparated flow into the fan. The rotor centre line was 2 m from the floor, in an arrangement similar for compact cooling fans. The authors acoustically treated the downstream and upstream plena, which connected the fan to the outside environment, to minimise both incidental noise from the induced air stream, and external noise transmission from the outside environment. A louver in the top of the facility's inlet section enabled the authors to make variations in both the fan head and flow rate. With the far-field microphone set at the same height as the rotor centre, the authors measured far-field noise at a distance of two fan diameters from the outflow sections (Leggat & Siddon, 1978), in accordance with the prescribed BS 848 standard for far-field noise testing in a semi-reverberant environment (ISO 2000).

Fig. 3. Test-rig and instrumentations

The authors measured the noise at several azimuthal locations from -90° to +90° from the rotor exhaust centre line with an angular increment of 30°. Air-speed measurements at the far-field microphone recorded negligible effects for all microphones.

### 4.2 Noise source dissection

The causal analysis utilises simultaneous measurements of the hydrodynamic pressure in the near-field and of the acoustic pressure in the far-field to separate aerodynamic noise sources at fan outlet. The authors based the adopted experimental technique in the present study, to varying degrees, on previous fan (Leggat & Siddon, 1978; Bianchi *et al.*, 2009b), radial pumps (Mongeau *et al.*, 1995), and turbofan engines (Kameier & Neise, 1997; Miles, 2006) studies. The experimental technique consisted of a pressure-field microphone traversing the blade's span with simultaneous pressure measurements in the far-field. The authors simultaneously recorded the signals from the near-field microphone and the far-field microphone on two separate channels of a 01-dB Symphonie digital signal processor.

The use of a cross correlation technique during data analysis enabled isolation of the near-field noise sources' signature from the far-field noise signal, thus avoiding error due to 'pseudo sound' (defined as turbulence-generated noise that a recording can pick up in the near-field, but which decays so quickly that it cannot be responsible for noise emission to the external environment). Correlation revealed a causal relationship between individual noise-source phenomena and the overall radiated sound in a given direction, thereby yielding quantitative information about the distribution of acoustic sources, their local spectra, and the degree of coherence. If a strong harmonic coupling between source and far-field spectra existed, it was apparent that the resulting correlation function did not decay quickly, but was periodic in nature.

Concerning the location of the near-field probe, the limit of the causal analysis in the present work is that all the measured aerodynamic sources in the near-field larger than the correlation length resulted in poor matching with the far-field and the cross-correlation did not highlight. Notably, the rotor blades under scrutiny operate with a tip-

based Reynolds number range of order $7.0\times10^5$, typically featuring an irregular vortex shedding. In agreement with numerous investigators who have reported on the correlation length dependence on flow conditions (Blake 1986), in a Reynolds number range $3.3\times10^3$ to $7.5\times10^5$ the correlation length is proportional to the length scale of the shed vortices $d$ i.e. $\Lambda_3 \approx d/2$. Past numerical studies in axial flow fans (Corsini *et al.*, 2009b) showed $d$ to be 10% to 20% of the blade span, when referring to the vortices shed by rotor blade passages. Accordingly, the value of the correlation length in the present test configuration is $\Lambda_3 \approx 7\%$ of the blade mid-span chord. In order to fulfill the correlation length threshold, the authors mounted the near-field test-rig setup microphone at 10% of the mid-span chord from the blade trailing edge, on a 10-mm wide traversing arm which was capable of moving the microphone along the whole blade span. The probe traversed the blade span in constant steps, each of which was 2% of the blade span. A rubber panel isolated the traversing arm from vibration in the chamber. During the measurements, a nose-cone windshield protected the microphone diaphragm, upon which the authors conducted a preliminary test to quantify its self-induced noise and thus enabled them to include a correction factor in data-processing calculations. The acoustic effects compensated for the measurement technique that the near-field microphone presence induced (Bianchi *et al.*, 2009b).

With the far-field microphone set at the same height as the rotor centre, the authors measured far-field noise at a distance of 2.3 fan diameters from the outflow section. Air-speed measurements at the far-field microphone recorded negligible airflow for all of these microphone positions, with the exception of the one at 0°. At such a distance, as Leggat & Siddon (1978) also found, we can ignore the direct influence of the flow over the microphone. Moreover, the researchers corrected for wind noise using a correction factor that the microphone manufacturer provided (Brüel & Kjær, 2006).

## 5. Experimental investigations

The aim of the family of blades experimental investigations which the authors designed according to the proposed synergistic passive noise control concepts, is to speculate on their aeroacoustic pay-off. The authors explore the nature of the noise-to-flow productive linkage by investigating the space distribution of the noise's directivity pattern and within the rotor blade span in the near-field. The presentation of the experimental findings includes: (i) integral Lp analysis of the directivity for the different configurations; (ii) spectral analysis of directivity of the rotor noise sources in the radiated field; and (iii) a description of the near-field sources responsible for the aerodynamic noise along the blade span.

The authors examined the fan's acoustic performance when fitted with each of the three blade-tip configurations (*datum*, TF, TFvte, TFmvb) under near-design operating conditions, with a volume flow rate of $V = 7\ m^3/s$.

### 5.1 Overall noise emission and directivity

The authors derived the Lp auto-spectra of the instantaneous pressure signals in the far-field under the tested operating condition, and then integrated it to calculate the Lp's azimuthal radiation patterns at seven angular positions on the rotor axis plane. Figure 4 shows the integrated Lp value of the *datum* fan plotted against those of the rotors fitted with the end-

plates. It is evident that the peak levels aligned with the fan axis for the *datum,* TF and TFvte fans. Remarkably, the TFmvb fan features a nearly isotropic radiation pattern with a large attenuation (as compared to all the other fan blades) of the axial level. As expected (Leggat & Siddon, 1978), the maxima in the near-axis direction for the *datum*, TF and TFvte fans indicated a significant dipolar noise source in the fan outlet. In the near-axis region, TF had a maximum Lp level of 82 dB, similar to the *datum* and the TFvte maxima (81 dB); whereas, the TFmvb peak was at 71 dB. According to previous directivity studies in a different test-rig set-up (Bianchi *et al.*, 2011a), the tendency toward the attenuation of in-axis noise correlated with the presence of coherent swirling structures in the exhaust flow. TFvte noise control design is even more magnified in the TFmvb end-plates.

When moving away from the fan axis, all the directivity patterns of the modified impellers differed from that of the *datum* fan. While the *datum*, the TF and the TFvte fans featured a dipolar-like emission, the TFmvb directivity confirmed its isotropic radiation. In a jet-noise sense, the TFmvb far-field directivity is a consequence of the shifting of low frequency noise sources (radiating axially) to the high frequency range (radiating laterally) which we can consider as the acoustic counterpart of the control implemented on the tip leakage vortex (enhanced mixing) and shed vorticity (reduction of 3D blade separation). This interpretation is routed on the causal relationship between small-scale random turbulent structures and high-frequency sound with nearly-isotropic radiation, and large-scale coherent eddies with directional patterns according to their frequency scales.

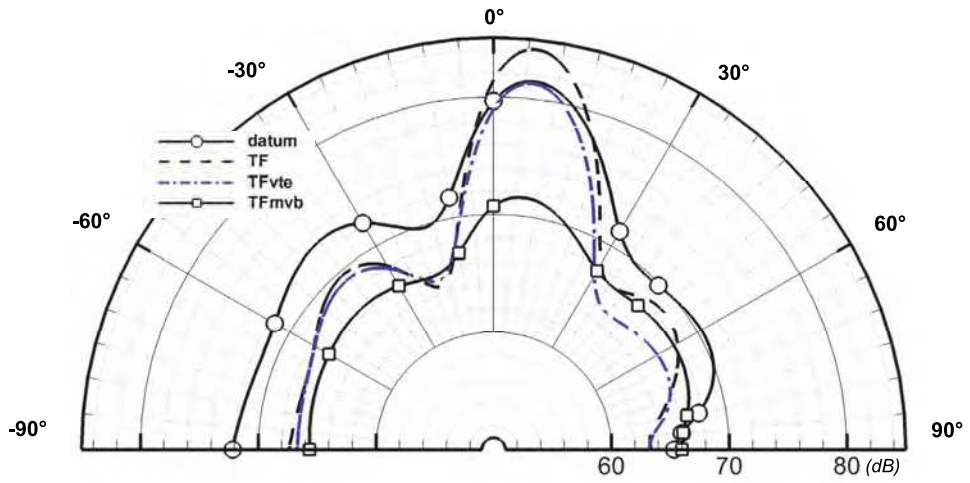


Fig. 4. Directivity of the integrated Lp for the different blade geometries.

The analyses showed that the dipolar noise characteristic of the *datum*, and original TF rotors changed in the TFmvb as a result of the superposition of reduced intensity longitudinal dipole and a lateral quadrupole. As Shah *et al.* (2007) previously stated, we can attribute this quadrupole-like noise source to the turbulent mixing of the swirling core flow which scatters the dipolar source related to the presence of a coherent vortical structure.

To give additional hints on the overall acoustic performance, Figure 4 shows polar diagrams correlating the A-filtered sound power level (LwA) and the specific noise level

(Ks) when varying the airflow power in the fan operating range. We define the specific noise level as Ks = Lw – 10 log[$V$ ($\Delta p_{tot}$)$^2$] (dB). The polar representation clearly shows the pay-off in the noise emission of the TFmvb, when compared with the datum and the TF and TFvte rotors.

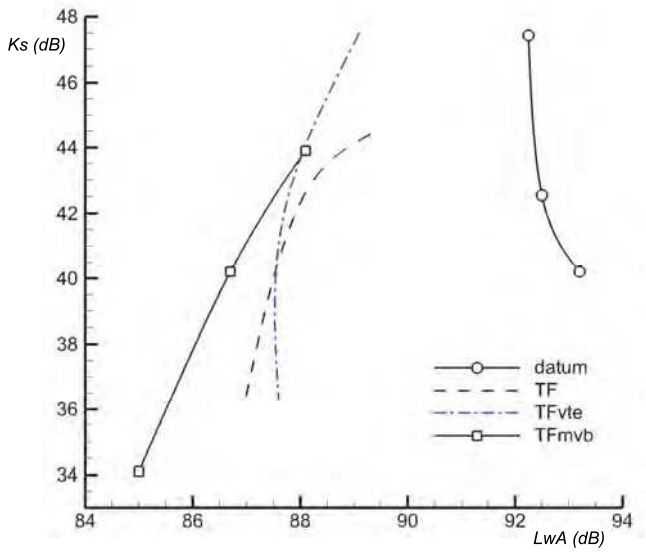


Fig. 5. Comparison of A-filtered overall sound power level (LwA) – specific noise level (Ks) polar plot.

Notably, the *datum* fan features a unique behaviour entailing, when increasing the power, a specific noise level reduction and an augmented sound power level, LwA. This suggests that the increased aerodynamic share in the sound generating mechanism, due to the actual fan operations, radiates more efficiently to the far-field and enhances the emitted noise in the audible frequency range. In contrast, both the fan blade fitted with end-plates show a difference on the sound power-specific power levels. In particular, the TF end-plate shows that the reduction of specific noise level with aerodynamic power correlates to an attenuation of the emitted noise according to a power law Ks $\propto$ (LwA)$^n$ with n = 0.5. Instead, the TFmvb speeds-up the reduction in sound levels featuring a nearly linear distribution of exponent n = 1.

### 5.2 Fourier analysis

In order to give additional hints on the directivity of noise spectra, Figure 5 compares the Lp narrow-band auto-spectra at three azimuthal positions in the far-field, namely 30° (top), 60° (mid) and 90° (bottom) angles to the fan axis. The authors mapped the Lp spectra in the frequency range 25 Hz to 10kHz.

It was confirmed that the noise radiation had a specific directional characterisation, irrespective to the particular geometry, both in the tonal noise and in the broadband components. The authors recorded the major acoustic emissions as expected, near the fan centre-line in the 30° position, in accordance with the dipolar-like noise signatures from early studies on low-speed fans (Wright, 1976) (Leggat & Siddon, 1978). Clearly, as the noise direction path moves farther from the axis line, two phenomena became evident: i) the Lp attenuation is mostly concentrated above 1 kHz, and ii) some of the fans featured an spectral tone noise enrichment as the aerodynamic broadband noise reduced its influence and allowed the tonal sources to emerge.

The directivity map of the Lp far-field autospectra at 30° shows that that all the tested fan blades, with the exception of the TFmvb one, had similar spectral behaviour with a plateau from the second fundamental harmonic to 1 kHz and in the narrowband where the only remarkable difference is the presence of emerging tones for the datum Lp over the tenth BPF. The TFmvb spectrum, on the opposite, featured an amplification of the second BPF, usually considered as a signature of the tip leakage vortex self-noise. Here the Lp of the TFmvb was 7 dB higher than the TF, and more than 10 dB higher than *datum* and TFvte. TFmvb tones were also evident on the third and the sixth BPFs which coincide with equivalent TF end-plate peaks. In the high frequency range, the TFmvb featured a steeper Lp attenuation (6 dB/kHz against 3.2 dB/kHz for the other blade geometries in the range 1kHz to 4 kHz). Moreover, the spectrum suddenly lose the higher harmonic tones in contrast to TF and TFvte spectra where tonal components emerge up to 8 kHz.

Similar noise frequency distribution appeared for the microphone at 60°. Nonetheless, there are noticeable small differences: i) a general reduction in the global noise level, ii) a further enrichment of the noise's tonal structure, and iii) the occurrence of an abrupt rise of Lp in the TF distribution above 5 kHz. Moving to the side of the fan exhaust at 90°, the Lp spectra changed remarkably, over the entire frequency range, in terms of Lp magnitude (i.e. at 1 kHz, Lp levels are comparable to those recorded at 30°) and broad-band attenuation.

In the spectra's low frequency portion, the TFmvb again featured a dominant tone on the second and third BPFs, with some degree of similarity to the TF spectrum only. Notably, after 300 Hz, the TFmvb spectrum lost any significant tonal behavior. The authors found similar spectra modifications in the broad-band at frequencies higher than 1 kHz for the *datum* and the TFvte. A different behavior was evident in the TF Lp spectrum, which again featured a significant rise in the broad-band. The authors attributed this noise increase to a particular phenomenon that they had studied in the TF fan (Corsini et *al.*, 2010). Close to the TF blade' trailing edge, the tip-leakage vortex collapsed and produced a 'bubble-type' separation that indicates vortex breakdown. The separated flow turned into a counter clockwise vortex under the influence of trailing-edge leakage flow streams. This results in a noise emission increase in the frequency range of interest as a consiquence of chaotic turbulent flow which is usually located in the mid-high frequency range.

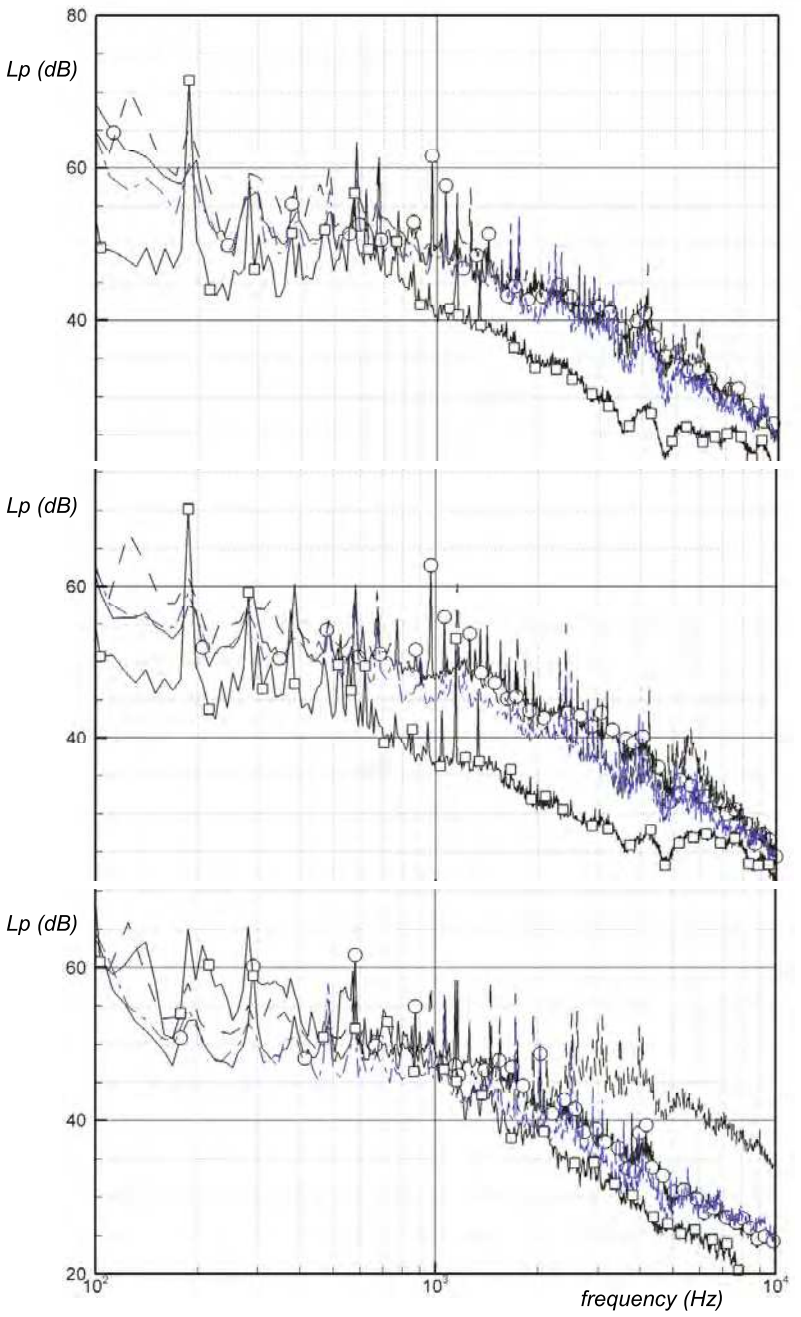


Fig. 6. Auto-spectra of the Lp for the different blade geometries at three azimuthal position: 30° (top), 60° (mid) and 90° (bottom)

The authors then calculated the Lw and Lw(A) power spectra which Figure 6 shows. The Lw spectra (Figure 6, top) demonstrated that, when integrating the pressure on the whole hemisphere, the noise that the different geometries emit for frequencies lower than 1 kHz likely had the same power level. In particular, the Lw spectra show distinctive features on the overall tonal behaviour, up to the 10th BPF harmonic. Notably, Figure 6 shows a differentiation of the *datum* from the rotors' spectra fitted with the end-plates, which gave evidence of background noise power level reduction and of the broad band noise level (about 10 dB difference to the *datum*). Concerning the A weighted noise power level (Figure 6, bottom), the differences are even more little. TF and TFvte spectra are pretty much super-positioned and they showed minimal differences in the emitted LwA. The TFmvb is similar to them for frequencies up to 1 kHz and then became quieter. Usually it was 10 dB quieter than the others, at the average, up to -14 dB in frequencies less than 5 kHz and -8 dB for the frequencies up to 10 kHz.

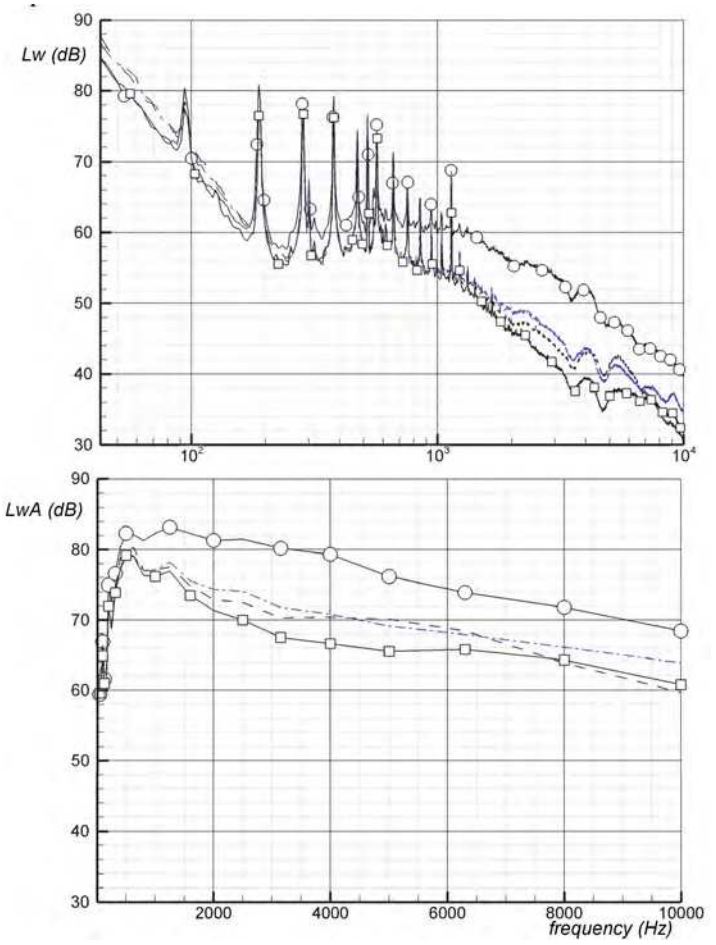


Fig. 7. Comparison of Lw (top) and LwA (bottom) for the different blade geometries

The authors undertook identification of noise sources in the flow exiting the fan rotor (as fitted with the various proposed end-plates) by using a coherence analysis, in the way that Bianchi *et al.* (2011b) recently developed. The coherence function ($\gamma$) involves a normalisation by frequency band that tends to highlight highly coherent events independently from their energy content. For this reason it is an effective mean of investigating near- to far-field acoustics, providing a resolution in noise space in the source regions. The authors plotted the coherence between the near-field and far-field microphone as a function of the radial position r and the non-dimensional frequency $\Im$, defined as *f/BPF*. Figure 8 illustrates, first, the coherence function's spanwise map for the rotor geometries at 30°. Similarly, Figures 9 and 10 present coherence distribution at 60° and 90° respectively, for the considered rotor geometries: *datum*, TF, TFvte, and TFmvb. The authors set the coherence threshold at $\gamma = 0.25$, as given by the anechoic room coherence response (Leggat and Siddon (1978) proscribed this value). The authors compared all four blade configurations (*datum*, TF, TFvte, and TFmvb) under near-design operating conditions.

The position at 30°, Figure 8, was closer to the fan axis and should be the one more influenced by the rotor discharged flow noise. The *datum* rotor map inferred about the blade-correlated noise sources, discriminating those capable of radiating downstream, thus affecting the progressive far-field. Some distinguished peaks of high coherence characterised this rotor along the whole span at $\Im = 6$ and at $\Im = 7$ and other tones which radiated mostly from the blade's inner part at $\Im = 3$ and at $\Im = 4$. The coherent tone at $\Im = 5$ appeared to correlate to the sources radiating from the hub to mid-span, together with the inter-tonal coherence between $\Im = 6$ - 7. Moreover, *datum*'s map also provided evidence of non-tonal coherent phenomena governing the far-field emission mechanisms in the blade tip's proximity and at the rotor hub. The first coherence region, mainly concentrated in the region from mid-span to tip for a range of $\Im = 3$ - 5, indicated a noise source related to the interaction between the tip-clearance vortex and the rotor wake in the region of highest load as a result of the blade design. At the blade root, in a similar frequency interval that is now slightly larger, $\Im$=3–7, the coherence iso-lines concentration indicated a second aerodynamic noise source caused by a hub corner stall interacting with the passage vortex.

It was possible to isolate coherent patterns attributable to specific tip vortex from the TF rotor map. The TF coherence map identified some differences from the *datum* one, which were apparently related to the aeroacoustic gains that Corsini *et al.* (2009b) previously studied. At higher radii, the TF end-plate appeared to cancel the coherence of tones, with the exception of the hub-corner interaction, which was only reduced, resulting in coherence loss in the region where the tip leakage vortex played the major influence on noise. Examination of the interaction noise cores showed that the region up to $\Im = 6$, appeared inefficiently radiated due to the reduced coherence. However, at about the sixth BPF harmonic, the authors found tonal-like coherence peaks, which, according to their radial position and frequency range, could relate to the tip-leakage vortex bursting that Corsini and Sheard (2007) detected in previous studies of this configuration under these operating conditions. The TF coherence map also showed evidence of a change in the non-tonal noise emission in the rotor hub's region. The coherent region's reduced extension, in terms of radii and frequencies, was in accordance with the control of secondary flows that attenuation of the near-surface fluid centrifugation produced.

The TFvte end-plate coherence distribution confirmed the test results of the constant-thickness tip concept. In particular, this configuration demonstrated an ability to eliminate

the coherence from the tones (remarkably, on the range of low $\Im$) at the tip and to decrease coherence due to tip-flow interaction noise sources. In addition, at the hub, this end-plate was capable of reducing the emission effectiveness from the secondary flow noise sources. Finally, the variable-thickness end-plate, owing to its design concept, reduced the extent and coherence level in the vortex breakdown radial and frequency ranges as a consequence of control of leakage vortex rotation.

The TFmvb end-plate revealed that the sequence of positive and negative *momentum* resulted in specific pattern that clearly distinguished these configurations from the original TF and TFvte configurations. First, both TFmvb and TFvte enhanced tone coherence, but reduced coherence with respect to the tip leakage interaction sources (in the range $\Im$ =3–5). Second, the application of multiple vortex breakdown concept on the end-plate configuration outperformed all the other configurations in reducing the breakdown noise correlation in the region about $\Im$ = 3. These findings provided evidence that the mechanism of the multiple vortex breakdown configurations consisted of: (i) acting as a mixing enhancer in the tip-leakage region; and (ii) then increasing the degree of scattering of the local noise sources.

Figure 9 compares the coherence of the instantaneous pressure/noise correlation of the four rotors at $\alpha$ = 60°. This measurement confirmed the previous behaviour, as Figure 7 indicates, for all the geometries and the coherence shape of the noise sources did not appear to change. The only difference was that the authors found specific traces of ingested noise (low frequency number range) in all the three rotors from the inlet plenum and in the signature of the rotor-only noise. With regard to this source, the authors found it to influence coherence on the first frequency number (spanning from the hub to the tip), irrespective of the tested tip configuration. Figure 9 then provided evidence of non-tonal coherent phenomena governing the far-field emission mechanisms in the low frequency which radiated exclusively to this angular pattern.

Finally, Figure 10 shows the coherence maps for $\alpha$ = 90°. In the narrowband at frequencies lower than the frequency number associated to the BPF ($\Im$ = 0.25 and 0.66), the authors also identified the rotor-alone noise. According to Cumpsty (1977), the existence of such a low-frequency tone is a noise source directly correlated to the upstream flow distortions that the rotor produces. The rotor presence in the duct usually causes the noise sources, without distinction whether the rotor spins or not. To support the evidence of ingested flow noise, Figure 10 represents coherence spectra near the *datum*. The analysis of Figure 10 suggested a maximum correlation was for the sources at very low frequency, located close to the hub and influencing the whole span. This observation infers that the noise already in the $\Im$ = 60° was an ingested noise. The path of this distortion then interacted with the rotor's bottom part and its tone was partly scattered to the high frequency broadband. Although these sources are present in all the geometries, as their cause is something excited by the blade's dynamic effects, the *datum* rotor showed to have less control of these low frequency noise sources. This is because the end-plates control the flow path along the blade, making possible a purely 2D flow span distribution, due to the flow blockage which the end-plate at the tip operates. In more detail, whilst the TFmvb reduced the tones to only one, but produced along all the blade span, the TF and, even better, TFvte also reduced the coherence of the remaining unique source. The rotor alone noise tone in the TF and TFvte geometries were so concentrated mainly in the tip zone and showed a possible, more effective, control of these end-plates on the flow distribution along the span with the consequence of reducing the noise excitation of the blade's bottom part with the incoming flow.

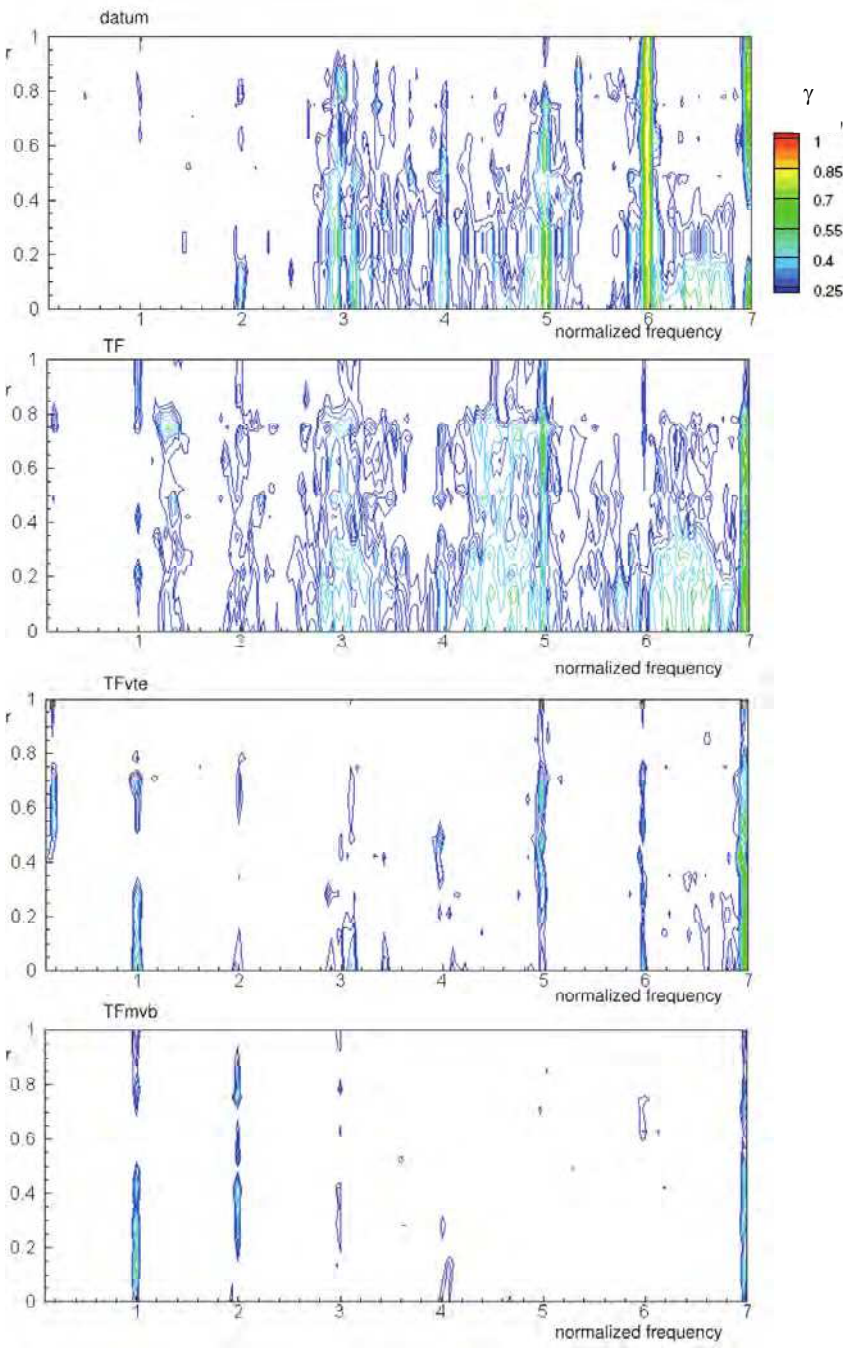


Fig. 8. Spanwise maps of coherence for the different blade geometries at 30°

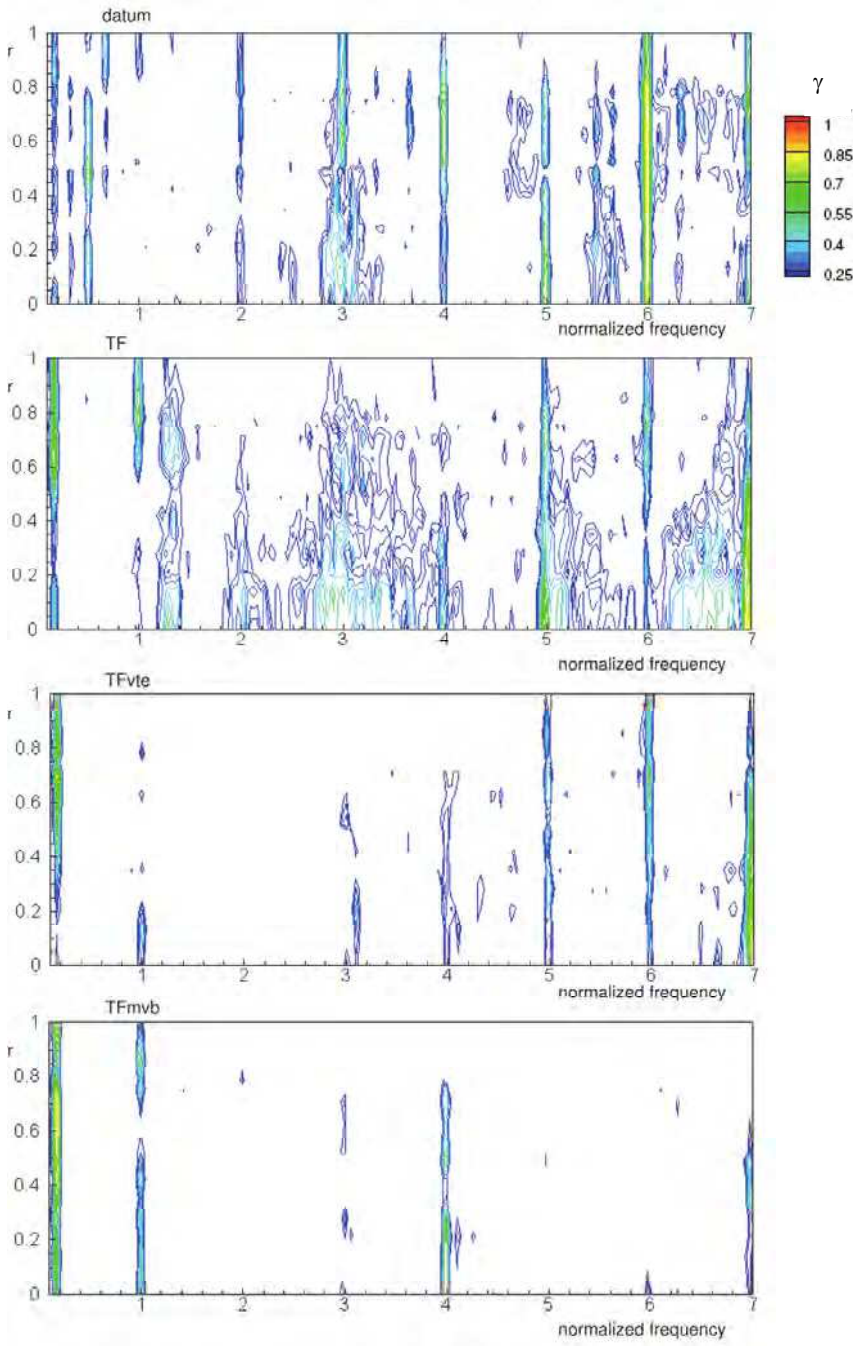


Fig. 9. Spanwise maps of coherence for the different blade geometries at 60°

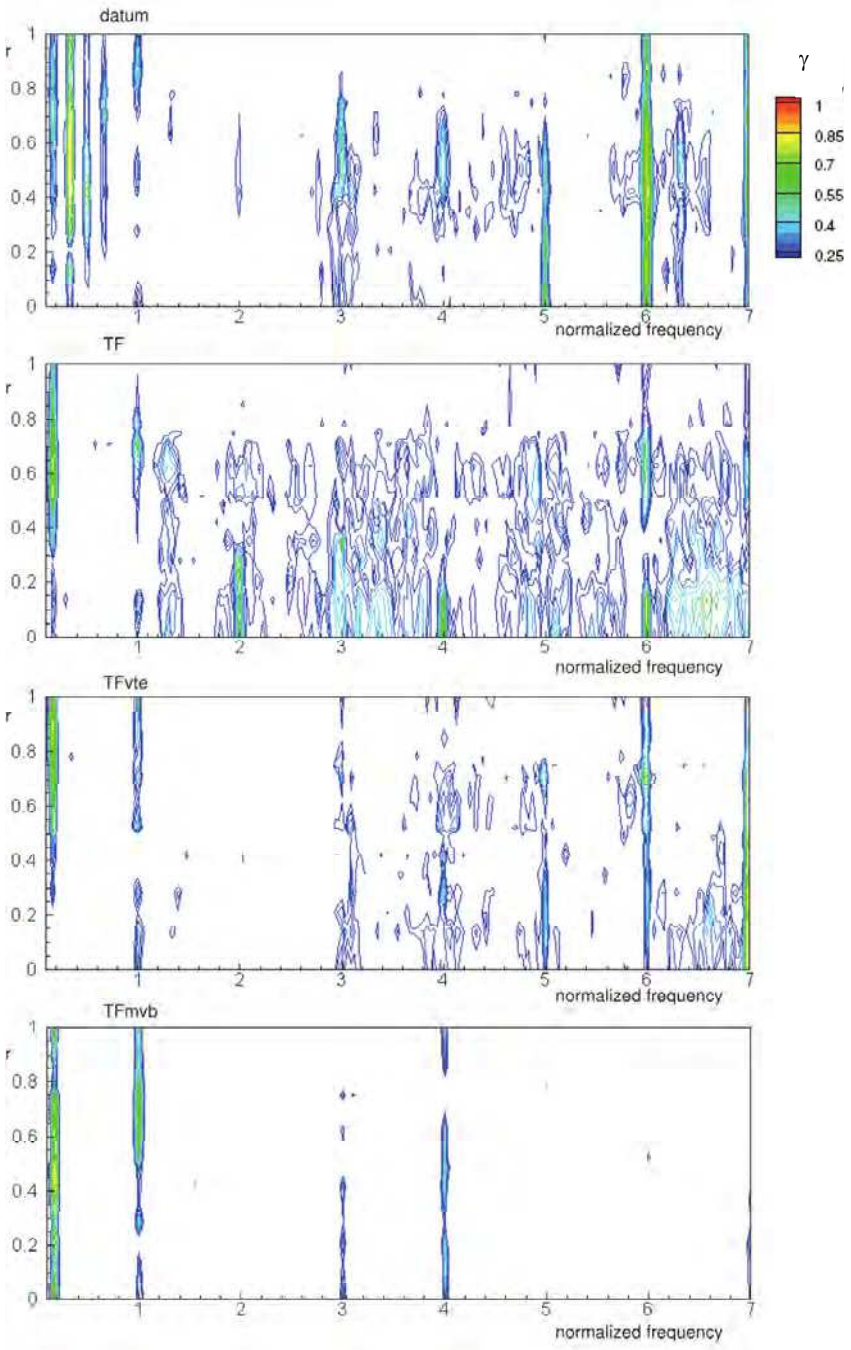


Fig. 10. Spanwise maps of coherence for the different blade geometries at 90°

## 6. Conclusions

The comparison of different tip features indicated a positive influence on the fan blades' global noise emission to which the authors applied them. The authors found that the end-plate tip geometry modifications reduced acoustic emission most significantly. The study demonstrates that the *datum* blade and the modified fixed-thickness ('TF' and 'TFvte') blades tip both associated with a directional noise emission that had its maximum Lp level in the fan outlet's centre line, thus producing a dipolar noise source. This behaviour has a slight impact on the broadband noise, with the broadband Lp general reduction associated with the TF configuration somewhat greater than that associated with the *datum* fan for the tip vortex breakdown occurrence. With regard to the multiple-vortex-breakdown ('TFmvb') tip concept, the experiments demonstrate that the directivity of the emitted noise changed, thus producing a pattern for this configuration that was more akin to a quadrupole-like source. The strongest component of this quadrupole-like source, which the authors suspect as a significant influence on the TFmvb noise emission, appears to emit in a direction of 90° degrees to the fan centre line, due to the ingested rotor alone noise.

The literature (Shah *et al.*, 2007) reports similar findings, and with this present study the authors can attribute this particular acoustic phenomenon to the tip leakage flow's augmentation of swirl level by means of end-plate shaping that promoted the coherent vortical structure occurence at an increased rotation rate spun at the fan rotor exhaust. These coherent vortical structures interact with the ingested rotor alone noise and thus excite the tones in low frequency in a completely different manner than the rotor with no end-plate. A near-far field "pressure to noise" correlation showed the presence of well defined aerodynamic sources acting to enhance noise enhanced and this, in agreement with the literature, was the cause of a different noise pattern that the modified geometries showed.

The signal correlations also showed the central importance of the low frequency and the influence of the blade tip noise in building the tonal harmonics. The data from the experiments demonstrated that the tip aeroacoustic emissions were sensitive to the rotor alone noise, but also that the end-plate control on the flow was beneficial in noise source reduction.

The results show the control feature of the TF, TFvte and TFmvb geometries on the tip derived noise, with respect of the *datum* blade. The auto-spectra in the broadband range also show a better control of the tip noise exhorted in this frequency range by the TFmvb. ,Past numerical investigation (Corsini *et al.*, 2009b, 2010) support the authors' asertion regarding the link existing between the broadband noise reduction and the tip flow peculiarities which TFmvb geometry features. The noise radiated by the TF family of impellers also shows a strong influence from a secondary source localised in the bottom part of the rotor. The TFvte and TFmvb blades also have an influence on this noise source, possibly because of the change that they produce on the whole flow circulation along the blade span.

## 7. Acknowledgment

The authors conducted the present research in the context of contract FW-DMA09-11 between *Fläkt Woods Ltd* and *Dipartimento di Ingegneria Meccanica e Aerospaziale, "Sapienza" University of Rome*.

## 8. References

BS 848-2.6:2000 (2000), ISO 10302:1996. *Fans for General Purposes. Methods of Noise Testing.*

ISO IEC60651, IEC/EN-61672-1. *Calibration Rules for Hardware in Noise Measurements.*

Akaike, S., Kuroki, S. & Katagiri, M. (1991), "Noise Reduction of Radiator Cooling Fan for Automobile: Three-dimensional Analysis of the Flow between the Blades of the Fan". *Society of Automotive Engineers of Japan*, vol. 22, pp 79–84.

Akturk, A. & Camci, C. (2010), "Axial Flow Fan Tip Leakage Flow Control using Tip Platform Extensions". *Journal of Fluids Engineering*, vol. 132, pp 101–10.

Akturk, A. & Camci, C. (2011a), "Tip Clearance Investigation of a Ducted Fan used in VTOL UAVS. Part 1: Baseline Experiments and Computational Validation". ASME Paper No. GT2011-46356.

Akturk, A. & Camci, C. (2011b), "Tip Clearance Investigation of a Ducted Fan used in VTOL UAVS. Part 2: Novel Treatments via Computational Design and their Experimental Verification". ASME Paper No. GT2011-46359.

Bianchi, S., Corsini, A., Rispoli, F. & Sheard, A.G. (2009a), "Experimental development of a measurement technique to resolve the radial distribution of fan aero-acoustic emissions". Noise Control Engineering Journal, vol. 57(4), pp 360-369.

Bianchi, S., Corsini, A., Rispoli, F. & Sheard, A.G. (2009b), "Detection of Aerodynamic Noise Sources in Low-speed Axial Fan with Tip End-plates". *Proceedings of the IMechE, Part C: Journal of Mechanical Engineering Science*, vol. 223, pp 1379–92.

Bianchi, S., Corsini, A., Rispoli, F. & Sheard, A.G. (2009c), "Experimental Aero-acoustic Studies on Improved Tip Configurations for Passive Control of Noise Signatures in Low-speed Axial Fans". *ASME Journal of Vibration and Acoustics*, vol. 131, pp 1–10.

Bianchi, S., Sheard, A.G., Corsini, A. & Rispoli, F. (2011a), "Far-field Radiation of Aerodynamic Sound Sources In Axial Fans Fitted With Passive Noise Control Features". ASME Journal of Vibration and Acoustics, vol. 133(5), paper 051001 (11 pages).

Blake,W.K. (1986), Mechanics of Flow-Induced Sound and Vibration, Vol. I.Academic Press, London, UK.

Brookfield, J.M. & Waitz, I.A. (2000), "Trailing Edge Blowing for Reduction of Turbomachinery Fan Noise". *AIAA Journal of Propulsion and Power*, vol. 16, pp 57–64.

Brüel & Kjaer (2006), *4954 ¼ inch Prepolarized Free-field Microphone Manual.*

Corsini, A., Rispoli, F., & Santoriello, A., (2005), "A Variational Multi-Scale High-Order Finite Element Formulation for Turbomachinery Flow Computations" , *Comput. Methods Appl. Mech. Eng.*, vol. 194 (45 – 47), pp 4797 – 4823.

Corsini, A. & Sheard, A.G. (2007), "Tip End-plate Concept Based on Leakage Vortex Rotation Number Control". *Journal of Computational and Applied Mechanics*, vol. 8, pp 21–37.

Corsini, A. & Sheard, A.G. (2011), "End-plate Design for Noise-by-flow Control in Axial Fans: Theory and Performance". Under revision in *Journal of Fluids Engineering*, manuscript reference number FE-11-1168.

Corsini, A., Rispoli, F. & Sheard, A.G. (2007), "Development of Improved Blade Tip End-plate Concepts for Low-noise Operation in Industrial Fans". *Journal of Power and Energy*, vol. 221, pp 669–81.

Corsini, A., Rispoli, F. & Sheard, A.G. (2009a), "A Meridional Fan". Patent Application No. WO/2009/090376.

Corsini, A., Rispoli, F. & Sheard, A.G. (2009b), "Aerodynamic Performance of Blade Tip End-plates Designed for Low-noise Operation in Axial Flow Fans". *Journal of Fluids Engineering*, vol. 131, pp 1–13, Paper No. 081101.

Corsini, A., Rispoli, F. & Sheard, A.G. (2010), "Shaping of Tip End-plate to Control Leakage Vortex Swirl in Axial Flow Fans". *Journal of Turbomachinery*, vol. 132, pp 1–9, Paper No. 031005.

Cumpsty, N.A. (1977), A Critical Reviewof Turbomachinery Noise. *Journal of Fluids Engineering*, vol. 99, pp 278–93.

Escudier, M. (1987), "Confined Vortices in Flow Machinery". *Annual Review of Fluid Mechanics*, vol. 19, pp 27–52.

Escudier, M., & Zehnder, N., (1982), "Vortex flow regimes", *Journal of Fluid Mechanics*, vol. 115, pp 105-121.

European Parliament (2005), *Directive 2005/32/EC Establishing a Framework for the Setting of Ecodesign Requirements for Energy-using Products and Amending Council Directive 92/42/EEC and Directives 96/57/EC and 2000/55/EC of the European Parliament and of the Council*.

Ffowcs Williams, J.E. (1977), "Aeroacoustics". *Annual Review of Fluid Mechanics*, vol. 9, pp 447–68.

Fukano, T., Takamatsu, Y. & Kodama, Y. (1986), "The Effects of Tip Clearance on the Noise of Low Pressure Axial and Mixed Flow Fans". *Journal of Sound and Vibration*, vol. 105, pp 291–308.

Furukawa, M., Inoue, M., Kuroumaru, M., Saiki, K. & Yamada, K., (1999), "The role of tip leakage vortex breakdown in compressor rotor aerodynamics", *Journal of Turbomachinery*, vol. 121, pp 469-480.

Gad-el-Hak, M. (2000), *Flow Control: Passive, Active, and Reactive Flow Management*. Cambridge University Press, Cambridge, UK.

Garg, A.K. & Leibovich, S. (1979), "Spectral Characteristics of Vortex Breakdown Flowfields". *Physics of Fluids*, vol. 22, pp 2053–64.

Herrada, M.A. & Shtern, V. (2003), "Vortex Breakdown Control by Adding Near-axis Swirl and Temperature Gradients". *Physical Review E*, vol. 68, pp 1–8.

Inoue, M. & Kuroumaru, M. (1989), "Structure of Tip Clearance Flow in an Isolated Axial Compressor Rotor". *American Society of Mechanical Engineers, Journal of Turbomachinery*, vol. 111, pp 250–6.

Inoue, M. & Furukawa, M., (2002) "Physics of tip clearance flow in turbomachinery", ASME paper FEDSM2002-31184.

Ito, T., Suematsu, Y. & Hayase, T. (1985), "On the Vortex Breakdown Phenomena in a Swirling Pipe-flow". *Nagoya University, Faculty of Engineering, Memoirs*, vol. 37, pp 117–72.

Jones, M.C., Hourigan, K. & Thompson, M.C. (2001), "The Generation and Suppression of Vortex Breakdown by Upstream Swirl Perturbations". *Proceedings of 14th Australian Fluid Mechanics Conference*. Adelaide, Australia.

Joslin, R.D., Rusell, H.T. & Choudhari, M.M. (2005), "Synergism of Flow and Noise Control Technologies". *Progress in Aerospace Sciences*, vol. 41, pp 363–417.

Kameier, F. & Neise, W. (1997), "Experimental Study of Tip Clearance Losses and Noise in Axial Turbomachines and their Reduction". *American Society of Mechanical Engineers, Journal of Turbomachinery*, vol. 119, pp 460–71.

Karlsson, S. & Holmkvist, T. (1986), "Guide Vane Ring For a Return Flow Passage in Axial Fans and a Method of Protecting It". Patent No. US 4,602,410.

Lakshminarayana, B., Zaccaria, M. & Marathe, B. (1995), "The Structure of Tip Clearance Flow in Axial Flow Compressors". *American Society of Mechanical Engineers, Journal of Turbomachinery*, vol. 117, pp 336–47.

Leggat, L.J. & Siddon, T.E. (1978), "Experimental Study of Aeroacoustic Mechanism of Rotor-vortex Interactions". *Journal of the Acoustical Society of America*, vol. 64, pp 1070–77.

Leibovich, S. (1982), "Wave Propagation, Instability, and Breakdown of Vortices". In Hornung, H.G. & Mueller, E.A. (eds), *Vortex Motion*. Vieweg, Braunschweig, Germany, pp 50–67.

Longet, C.M.L. (2003), "Axial Flow Fan with Noise Reducing Means". US Patent No. 2003/0123987 A1.

Longhouse, R.E. (1978), "Control of Tip-vortex Noise of Axial Flow Fans by Rotating Shrouds". *Journal of Sound and Vibration*, vol. 58, pp 201 – 14.

Lucca-Negro, O., & O'Doherty, T., (2001), "Vortex breakdown: a review", *Progress in Energy and Combustion Science*, vol. 27, pp 431–481.

Miles, J.H. (2006), "Procedure for Separating Noise Sources in Measurements of Turbofan Engine Core Noise". Report NASA/TM-2006-214352.

Mimura, M. (2003), "Axial Flow Fan". US Patent No. 6,648,598 B2.

Mongeau, L., Thompson, D.E. & McLaughlin, D.K. (1995), "A Method for Characterizing Aerodynamic Sound Sources in Turbomachines". Journal of Sound and Vibration, vol. 181, pp 369 – 89.

Quinlan, D.A. & Bent, P.H. (1998), "High Frequency Noise Generation in Small Axial Flow Fans". *Journal of Sound and Vibration*, vol. 218, pp 177–204.

Saiyed, N.H., Bridges, J.E. & Mikkelsen, K.L. (2000), "Acoustics and Thrust of Separated-flow Exhaust Nozzles with Mixing Devices for High-bypass-ratio Engines". AIAA Paper No. 2000-1961.

Shah, P.D., Mobed, D., Spakovszky, Z. & Brooks, T.F. (2007), "Aero-Acoustics of Drag Generating Swirling Exhaust Flows". *13th AIAA/CEAS Aeroacoustics Conference (28th AIAA Aeroacoustics Conference)*. Rome, Italy, Paper No. AIAA-2007-3714.

Smith, G.D.J. & Cumpsty, N.A. (1984), "Flow Phenomena in Compressor Casing Treatment". *Journal of Engineering for Gas Turbines and Power*, vol. 106, pp 532–41.

Spall, R.E., Gatski, T.B. & Grosch, C.E. (1987), "A Criterion for Vortex Breakdown". *Physics of Fluids*, vol. 30, pp 3434–40.

Srigrarom, S. & Kurosaka, M. (2000), "Shaping of Delta-wing Platform to Suppress Vortex Breakdown". *AIAA Journal*, vol. 38, pp 183–6.

Storer, J.A. & Cumpsty, N.A. (1991), "Tip Leakage Flow in Axial Compressors". *American Society of Mechanical Engineers, Journal of Turbomachinery*, vol. 113, pp 252–9.

Takata, H. & Tsukuda, Y. (1977), "Stall Margin Improvement by Casing Treatment: Its Mechanism and Effectiveness". *Journal of Engineering for Power*, vol. 99, pp 121–33.

Thomas, R.H., Choudhari, M.M. & Joslin, R.D. (2002), "Flow and Noise Control: Review and Assessment of Future Directions". NASA Report TM-2002-211631.

Thompson, D.W., King, P.I. & Rabe, D.C. (1998), "Experimental and Computational Investigation on Stepped Tip Gap Effects on the Flowfield of a Transonic Axial-flow Compressor Rotor". *Journal of Turbomachinery*, vol. 120, pp 477–86.

Uchida, S., Nakamura, Y. & Ohsawa, M. (1985), "Experiments on the Axisymmetric Vortex Breakdown in a Swirling Air Flow". *Transactions of the Japan Society for Aeronautical and Space Sciences*, vol. 27, pp 206–16.

Uselton, R.B., Cook, L.J. & Wright, T. (2005), "Fan with Reduced Noise Generation". US Patent No. 2005/0147496 A1.

Wright, S.E. (1976), "The Acoustic Spectrum of Axial Flow Machines", *Journal of Sound and Vibration*, vol. 45, pp 165–223.

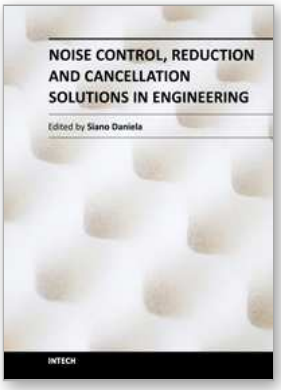


**Noise Control, Reduction and Cancellation Solutions in Engineering**

Edited by Dr Daniela Siano

ISBN 978-953-307-918-9
Hard cover, 298 pages
**Publisher** InTech
**Published online** 02, March, 2012
**Published in print edition** March, 2012

Noise has various effects on comfort, performance, and human health. For this reason, noise control plays an increasingly central role in the development of modern industrial and engineering applications. Nowadays, the noise control problem excites and attracts the attention of a great number of scientists in different disciplines. Indeed, noise control has a wide variety of applications in manufacturing, industrial operations, and consumer products. The main purpose of this book, organized in 13 chapters, is to present a comprehensive overview of recent advances in noise control and its applications in different research fields. The authors provide a range of practical applications of current and past noise control strategies in different real engineering problems. It is well addressed to researchers and engineers who have specific knowledge in acoustic problems. I would like to thank all the authors who accepted my invitation and agreed to share their work and experiences.

**How to reference**

In order to correctly reference this scholarly work, feel free to copy and paste the following:

Stefano Bianchi, Alessandro Corsini and Anthony G. Sheard (2012). Synergistic Noise-By-Flow Control Design of Blade-Tip in Axial Fans: Experimental Investigation, Noise Control, Reduction and Cancellation Solutions in Engineering, Dr Daniela Siano (Ed.), ISBN: 978-953-307-918-9, InTech, Available from: http://www.intechopen.com/books/noise-control-reduction-and-cancellation-solutions-in-engineering/synergistic-noise-by-flow-control-design-of-blade-tip-in-axial-fans-experimental-investigation

INTECH
open science | open minds

**InTech Europe**
University Campus STeP Ri
Slavka Krautzeka 83/A
51000 Rijeka, Croatia
Phone: +385 (51) 770 447
Fax: +385 (51) 686 166
www.intechopen.com

**InTech China**
Unit 405, Office Block, Hotel Equatorial Shanghai
No.65, Yan An Road (West), Shanghai, 200040, China
中国上海市延安西路65号上海国际贵都大饭店办公楼405单元
Phone: +86-21-62489820
Fax: +86-21-62489821